

# Boosting HDR Image Reconstruction via Semantic Knowledge Transfer

Qingsen Yan<sup>1\*</sup> Tao Hu<sup>1\*</sup> Genggeng Chen<sup>2</sup> Wei Dong<sup>2</sup> Yanning Zhang<sup>1†</sup>

<sup>1</sup>The School of Computer Science, Northwestern Polytechnical University

<sup>2</sup>Xi'an University of Architecture and Technology

## Abstract

Recovering High Dynamic Range (HDR) images from multiple Low Dynamic Range (LDR) images becomes challenging when the LDR images exhibit noticeable degradation and missing content. Leveraging scene-specific semantic priors offers a promising solution for restoring heavily degraded regions. However, these priors are typically extracted from sRGB Standard Dynamic Range (SDR) images, the domain/format gap poses a significant challenge when applying it to HDR imaging. To address this issue, we propose a general framework that transfers semantic knowledge derived from SDR domain via self-distillation to boost existing HDR reconstruction. Specifically, the proposed framework first introduces the Semantic Priors Guided Reconstruction Model (SPGRM), which leverages SDR image semantic knowledge to address ill-posed problems in the initial HDR reconstruction results. Subsequently, we leverage a self-distillation mechanism that constrains the color and content information with semantic knowledge, aligning the external outputs between the baseline and SPGRM. Furthermore, to transfer the semantic knowledge of the internal features, we utilize a semantic knowledge alignment module (SKAM) to fill the missing semantic contents with the complementary masks. Extensive experiments demonstrate that our method can significantly improve the HDR imaging quality of existing methods.

## 1. Introduction

Multiple-exposure High Dynamic Range (HDR) imaging aims to accurately recover images with a wide luminance range from exposure-varied Low Dynamic Range (LDR) images. However, LDR images are often captured in dynamic scenes, existing deep learning-based methods primarily focus on the aligned LDR sequences and fusing them to obtain high-quality HDR results [31]. Nevertheless, in practical scenarios, LDR images often suffer from noticeable degradation in dark scenes, while bright scenes may

\*The first two authors contributed equally to this work.

†Corresponding author.

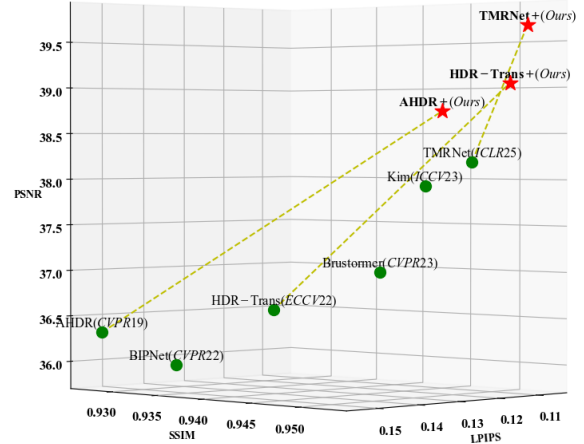


Figure 1. Performance comparison on the BracketIRE dataset, which consists of RAW format data pairs.

experience essential content misses due to occlusion caused by object movement. Despite advancements in recent network designs (e.g., CNNs [12, 25, 37, 49], Transformer-based methods [3, 22, 27, 28]), the inherently ill-posed nature of captured LDR images presents challenges in achieving substantial improvements solely through modifications to network structures.

Previous research [18, 32, 34, 45] has demonstrated the potential of using semantic priors to address ill-posed problems in low-level vision tasks. By integrating these priors, models can gain a deeper understanding of image content, providing explicit instructions that guide the reconstruction process. However, no work to date has explored this methodology specifically for multi-exposure HDR imaging. In current low-level vision tasks, the predominant approach [18, 32, 34] involves directly incorporating semantic priors derived from degraded images into the reconstruction network, thereby guiding the model to produce high-quality results. However, these approaches face significant challenges when applied to HDR imaging: First, existing prior extraction models are primarily designed for sRGB-format SDR images. The domain gap between HDR and SDR makes it difficult to yield high-quality priors for HDR imag-

ing, particularly some HDR datasets are stored in RAW format [52]. Second, even when suitable semantic priors are obtained, applying sRGB-derived priors to HDR images in RAW format introduces mismatches due to differences in data representation and dimensionality. Furthermore, HDR imaging relies on multiple LDR images with varying exposures, where semantic information can vary significantly across images, leading to incomplete or conflicting priors from each input.

The aforementioned issues motivate us to leverage semantic priors from another perspective. The motivation for our work is threefold. First, given the variations and conflicts in semantics within each LDR image, we exploit fused HDR images to extract high-quality semantic priors. To this end, we employ a pre-trained semantic segmentation network as a Semantic Knowledge Bank (SKB), which consists of semantic features and segmentation maps. Second, considering the domain gap between HDR and SDR, we perform prior embedding in the SDR domain to enhance the quality of the initial HDR results, fully harnessing the potential of semantic knowledge. Third, inspired by the semantic consistency across different formats and domains, we distill semantic knowledge from the SDR domain to boost the performance of existing HDR models.

Based on the above analysis, we propose a general framework that effectively leverages the advanced capabilities of semantic priors for HDR imaging. Specifically, our proposed framework comprises the Original Reconstruction Model (ORM), the Semantic Priors Guided Reconstruction Model (SPGRM), and the Semantic Knowledge Transfer Scheme (SKTS). The ORM can be any existing HDR imaging method, tasked with generating initial HDR results. The SPGRM utilizes intermediate semantic features derived from the SKB to refine the reconstructed image. Notably, the ORM operates in the HDR domain, whereas the SPGRM functions in the SDR domain. Subsequently, the SKTS exploits semantic consistency across formats/domains, using knowledge distillation [44] to ensure the ORM aligns with the semantic knowledge embodied in the SPGRM. Unlike existing distillation methods that solely distill priors in image content-level, we also introduce a Semantic-Guided Histogram Loss to enhance color consistency across distinct object instances. Furthermore, inspired by MAE’s masked reconstruction [8], we introduce a Semantic Knowledge Alignment Module to assist SKTS, ensuring consistency in the semantic feature space during the distillation process. As illustrated in Fig.1, our framework significantly enhances the performance of all baseline models. The main contributions can be summarized as follows:

- We propose a general semantic knowledge Transfer framework to boost the performance of existing HDR imaging models without modifying the original network.

- We propose three key techniques to take full advantage of semantic priors provided by the semantic knowledge bank: the Semantic Priors Guided Reconstruction Model, the Semantic-Guided Histogram Loss, and the Semantic Knowledge Alignment module.
- We conduct experiments on several RAW/sRGB format datasets, demonstrating that our method can significantly improve the HDR imaging quality of existing methods.

## 2. Related Work

**Multi-exposure HDR Imaging.** Traditional methods for multi-exposure HDR imaging primarily rely on preprocessing techniques (*e.g.*, motion rejection, motion registration) [9, 10, 26, 29, 33, 36] to align LDR images and reconstruct high-quality results. However, this approach heavily depends on preprocessing technologies and is less effective for large-scale object movements. In recent years, deep learning-based methods have emerged as a promising alternative, researchers have explored a variety of deep neural network (DNN) architectures and techniques. For instance, attention mechanisms [2, 37, 39] have been employed to selectively focus on relevant image regions, enhancing alignment and fusion accuracy. Similarly, transformer-based models [3, 21, 27, 28] leverage global contextual understanding to improve robustness in HDR reconstruction. Optical flow-based approaches [12, 14, 35] estimate motion between frames to compensate for misalignment, while generative adversarial networks (GANs) [24] and diffusion models [11, 40, 41] have been adapted to synthesize realistic HDR content from imperfect inputs. Additional innovative frameworks, such as [7, 47], further expand the scope of DNN applications in this domain. However, existing multi-exposure HDR imaging methods primarily focus on addressing artifact issues caused by motion, but they overlook the inherently ill-posed nature of captured LDR images in real-world scenarios. When LDR images contain noticeable degradations or information loss, their reconstruction quality is significantly reduced.

**Semantic Priors for Image Reconstruction.** Recently, methods that utilize semantic priors to guide image reconstruction in low-level visual tasks have proven effective in handling ill-posed problems. Semantic-loss-guided methods [1, 20, 51] employ semantic segmentation loss to explicitly enforce semantic segmentation capabilities within the model. This strategy enhances the model’s capacity to capture deep semantic features. Similarly, Wu *et al.* [34] and Liang *et al.* [18] utilize segmentation maps as priors to design tailored loss functions, thereby boosting overall model performance. In contrast, segmentation map [6, 32, 45, 51] and intermediate feature [16, 17, 34] guided methods share similar application strategies, differing only in the type of prior embedded within the model. SFTGAN [32] was one of the earliest methods to use semantic seg-

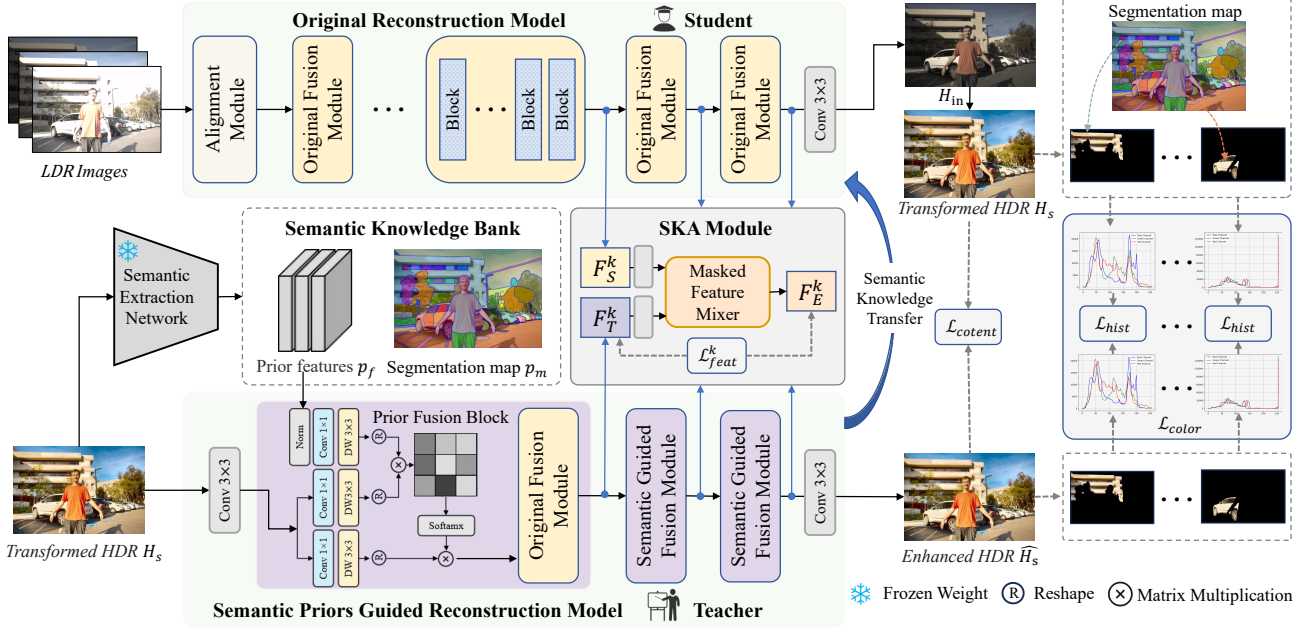


Figure 2. The Proposed Semantic Knowledge Transfer Framework. During training, the SPGRM enhances ORM’s initial HDR results by integrating semantic priors. Meanwhile, the Semantic Knowledge Transfer scheme boosts the performance of the ORM through model/feature-level self-distillation. During inference, only the optimized ORM is deployed, ensuring high efficiency.

mentation maps as priors to guide models in low-level visual tasks. Despite their success, existing semantic prior-guided methods are predominantly confined to the SDR domain. This limitation introduces a significant domain gap when extending these techniques to HDR imaging, especially given that HDR images are stored in RAW format. Bridging this gap remains a critical challenge for adapting semantic prior-guided approaches to HDR contexts.

### 3. Method

#### 3.1. Overview of Proposed Framework

As shown in Fig. 2, our framework primarily consists of the Original Reconstruction Model (ORM) and the Semantic Priors Guided Reconstruction Model (SPGRM), with knowledge self-distillation performed through the Semantic Knowledge Transfer Scheme (SKTS). Given a series of LDR images of a dynamic scene  $\{L_1, L_2, \dots, L_n\}$ , the ORM utilizes existing HDR reconstruction methods to produce the initial HDR images  $H_{in}$ . These initial HDR images are then converted into tonemapped sRGB domain results  $H_s$  through a domain transfer operation:

$$H_{in} = f_{org}(L_1, L_2, \dots, L_n; \theta_o), H_s = \mathcal{T}(H_{in}), \quad (1)$$

where  $\mathcal{T}(\cdot)$  represents the domain transfer operation, which for sRGB format data includes a  $\mu$ -law function, and for RAW format data additionally includes a differentiable demosaicing operation;  $f_{org}$  denotes the ORM network, and

$\theta_o$  is the network parameters. To extract semantic priors, the subsequent process can be represented as:

$$p_f, p_m = f_{seg}(H_s; \theta_s), \quad (2)$$

where  $p$  is the semantic prior, including segmentation maps  $p_m$  and intermediate features  $p_f$  with multi-scale dimensions.  $f_{seg}$  and  $\theta_s$  represents the pre-trained segmentation network and its frozen parameters. Then,  $p_f$  and  $H_s$  are used as inputs to the SPGRM to obtain the enhanced reconstruction result  $\widehat{H}_s$ :

$$\widehat{H}_s = f_e(H_s, p_f; \theta_e), \quad (3)$$

where  $f_e$  and  $\theta_e$  are the network and corresponding parameters of the SPGRM.

During the training stage, we use the SKTS to embed the semantic knowledge from  $f_e$  into  $f_{org}$  through the self-distillation manner.  $\theta_e$  and  $\theta_o$  will be updated by minimizing the objective function while  $\theta_s$  is fixed. During the inference stage, only  $f_{org}$  participates in the inference, without requiring  $f_e$  and  $f_{seg}$  to be involved.

#### 3.2. Semantic Priors Guided Reconstruction Model

To avoid semantic variations and conflicts in each LDR image, we utilize ORM’s result to extract semantic priors. However, when leveraging these priors to guide the model in reconstructing high-quality images, another challenge that requires careful attention is the disparity between

the prior and feature sources. To address this, we implement the SPGRM in the sRGB SDR domain, producing sRGB-tonemapped HDR results. Notably, the ORM and the SPGRM are trained simultaneously, and the transformation operation does not compress any of the original HDR content or impede gradient backpropagation.

As illustrated in Fig. 2, existing HDR imaging models typically follow an “align-then-fuse” paradigm, implicitly aligning LDR images before fusing them to produce HDR results. Given that the SPGRM takes the ORM’s results as input, it solely consists of three Semantic Guided Fusion Modules and excludes the LDR alignment module. In our framework, we employ FastSAM [50] as the SKB owing to its outstanding performance and ease of use. We leverage the output features before the representation head to get four multi-scale semantic features  $p_f^i \in \mathbb{R}^{C_i \times \frac{H}{2^{4-i}} \times \frac{W}{2^{4-i}}}$  ( $i = 0, 1, 2, 3$ ). Here,  $C_i$  represents the channel dimension, and  $H$  and  $W$  denote the height and width of the input image, respectively. These  $p_f^i$  features are processed through a Feature Pyramid Network (FPN) [19] for multi-level feature interaction, yielding  $p_f$ , which is adjusted to match the channel dimensions of SPGRM’s intermediate features. To incorporate the semantic priors  $p_f$ , we add a Prior Fusion Block to generate the refined feature map  $F_k^T$  within each fusion module. Specifically, as depicted in Fig. 2, the Prior Fusion Block takes two inputs: an intermediate feature  $F_k^T$  and a prior feature  $p_f$ . We project  $p_f$  into a query vector  $Q = W_d^Q W_c^Q p_f$  using point-wise  $1 \times 1$  convolution and depth-wise  $3 \times 3$  convolution with weights  $W_d^Q$  and  $W_c^Q$ , respectively. Similarly,  $F_k^T$  is transformed into Key  $K$  and Value  $V$  through analogous operations. Then, we adopt a transposed-attention mechanism [43] to compute the attention map. Hence, the process can be described as follows:

$$\bar{F}_k^T = W_c V \cdot \text{Softmax}(K \cdot Q / \gamma) + F_k^T, \quad (4)$$

where  $\gamma$  is a trainable parameter.

### 3.3. Semantic Knowledge Transfer Scheme

During the initial training phase, the output of SPGRM produces a high-quality tone-mapped HDR image  $\widehat{H}_s$ , which incorporates semantic priors and exhibits improved image quality compared to the initial HDR image  $H_{in}$ . To bridge this performance gap and enable the ORM to match or approximate the SPGRM’s capabilities, we introduce a semantic knowledge transfer scheme, which utilizes SPGRM as a teacher signal to guide the training of the ORM. The key aspects of the scheme are as follows:

**Preliminary alignment.** When utilizing the SPGRM as the teacher model, a critical challenge arises from disparities in the outputs, including domain mismatches (e.g., HDR vs. SDR) and representation differences (e.g., RAW vs. sRGB), between the SPGRM and ORM. To address

this challenge, we propose a simple yet effective approach: before performing self-distillation, we introduce a domain transfer operator  $\mathcal{T}(\cdot)$  to align the outputs of the two models across domains and representations. Provided the transfer function is reversible and differentiable, optimizing the network in the transformed domain implicitly boosts the student model’s performance. Notably, the transformation operation does not compress any of the original HDR content or impede gradient backpropagation.

**Semantic Knowledge distillation.** Unlike previous work that focuses solely on knowledge distillation at the content level, we recognize the importance of color alongside content in HDR reconstruction tasks. Therefore, our scheme executes knowledge transfer at both the content and color levels. For the content level, we distill the semantic priors from the SPGRM to the ORM by minimizing the  $\mathcal{L}_1$  loss in pixel space and the perceptual loss in the feature representation space:

$$\mathcal{L}_{content} = \|\mathcal{T}(H_{in}) - \widehat{H}_s\|_1 + \lambda \|\phi_{i,j}(\mathcal{T}(H_{in})) - \phi_{i,j}(\widehat{H}_s)\|_1, \quad (5)$$

where  $\mathcal{T}(\cdot)$  denotes the domain transfer operator;  $\widehat{H}_s$  is the output of the SPGRM, and  $H_{in}$  is the output of the ORM.  $\phi_{i,j}(\cdot)$  signifies the  $j$ -th convolutional feature extracted from the VGG19 network after the  $i$ -th maxpooling operation, and  $\lambda = 1e - 2$  is a balance hyperparameter.

At the color level, unlike conventional color loss functions [48] that focus on global statistical properties, our approach tackles the significant brightness variations across different regions in HDR images by enforcing constraints on distinct object instances. Given the discrete nature of color histograms, we propose a Semantic-Guided Histogram Loss that leverages Kernel Density Estimation (KDE) [42] to compute a differentiable histogram. Specifically, we first define the bin centers of the histogram. For a total of  $N$  bins, the center of the  $i$ -th bin  $c_i$  is computed as:

$$c_i = \min + \frac{\max - \min}{N} (i + 0.5), \quad i \in \{0, \dots, N - 1\}, \quad (6)$$

where  $\max$  and  $\min$  represent the upper and lower bounds of the pixel values, respectively. Let  $x_{c,j} \in \mathbb{R}^{3 \times H \times W}$  denote the  $j$ -th pixel value in the  $c$ -th channel of the input image. The Gaussian kernel value between  $x_{c,j}$  and the  $i$ -th bin center  $c_i$  is computed as:

$$K(x_{c,j}, c_i) = \exp\left(-\frac{(x_{c,j} - c_i)^2}{\sigma^2}\right), \quad (7)$$

where  $\sigma=400$  is the bandwidth parameter. The approximate histogram value  $H_{c,i}$  of the  $c$ -th channel is:

$$H_{c,i} = \sum_{j=1}^{H \times W} K(x_{c,j}, c_i). \quad (8)$$

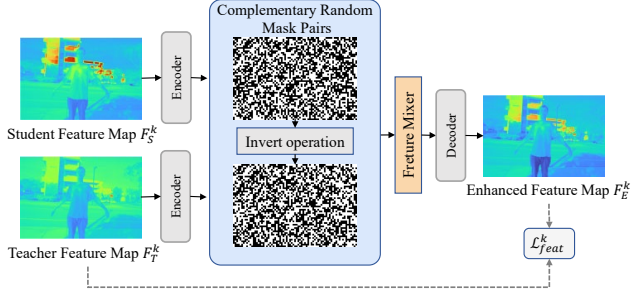


Figure 3. The process of Semantic Knowledge Alignment Module, which conducts semantic knowledge transfer at the feature level.

Then, the MSE loss between the two histograms is used as the histogram loss:

$$\mathcal{L}_{\text{hist}} = \frac{1}{C} \sum_{c=1}^C \sum_{i=0}^{N-1} (H_{c,i}^S - H_{c,i}^T)^2, \quad (9)$$

where  $H^S$  and  $H^T$  represent the color histograms of the student and teacher model’s outputs, respectively. Building on Eq. (9), the proposed  $\mathcal{L}_{\text{color}}$  is formulated as:

$$\mathcal{L}_{\text{color}} = \frac{1}{N} \sum_{i=0}^{N-1} \text{Hist} \left( p_m^i \odot \mathcal{T}(H_{\text{in}}), p_m^i \odot \widehat{H}_s \right), \quad (10)$$

where  $\odot$  denotes element-wise multiplication,  $p_m^i$  is the  $i$ -th channel of the segmentation maps derived from SKB, and  $\text{Hist}(\cdot)$  is the histogram loss computed over each region.

### 3.4. Semantic Knowledge Alignment Module

Beyond model-level distillation, semantic transfer at the feature-level is equally essential. However, since the ORM and SPGRM operate in different domains or formats, directly aligning their features can impair model performance. To address this issue, we introduce the Semantic Knowledge Alignment Module (SKAM), which progressively enhances semantic knowledge consistency at the feature-level within a unified latent space.

The motivation behind SKAM is twofold. First, since different domains/formats share the same semantic information, knowledge transfer of feature-level can be achieved within a unified latent space. Second, inspired by the masked reconstruction [15], we aim to perform feature-level distillation in a more gradual manner, rather than directly minimizing feature distances. Specifically, as shown in Fig. 3, SKAM comprises two encoders, a masked feature mixer, and a decoder. At the  $k$ -th alignment stage, feature maps from the ORM ( $F_S^k$ ) and SPGRM ( $F_T^k$ ) are processed by their respective encoders, mapping them into a unified latent space to produce latent representations  $\widehat{F}_S^k$  and  $\widehat{F}_T^k$ . These representations are then blended using a pair

of randomly generated complementary masks. The decoder subsequently transforms the combined features into an enhanced feature  $F_E^k$  in the same space as  $F_T^k$ , expressed as:

$$F_E^k = \text{Decoder} \left( \widehat{F}_S^k \odot (\mathbf{1} - \mathbf{I}^M) + \widehat{F}_T^k \odot \mathbf{I}^M \right), \quad (11)$$

where  $\mathbf{I}^M \in \{0, 1\}^{C \times H \times W}$  denotes a randomly generated binary mask, and  $\odot$  represents element-wise matrix multiplication. To minimize the semantic knowledge representation gaps between the ORM and SPGRM at the feature-level, the knowledge alignment loss is computed as:

$$\mathcal{L}_{\text{feat}}^k = \text{MSE} (F_E^k, F_T^k), \quad (12)$$

where MSE refers to the mean squared error.

### 3.5. Training and Inference

In the training stage, the SPGRM is exclusively supervised using a domain-transferred ground truth and optimized through an  $\mathcal{L}_1$  loss, denoted as  $\mathcal{L}_{\text{spg}}$ :

$$\mathcal{L}_{\text{spg}} = \left\| \widehat{H}_s - \mathcal{T}(GT) \right\|_1, \quad (13)$$

Meanwhile, the ORM is supervised using its original reconstruction loss functions, denoted as  $\mathcal{L}_{\text{org}}$ . The overall objective function for the ORM, denoted as:

$$\mathcal{L} = \mathcal{L}_{\text{org}} + \lambda_1 \mathcal{L}_{\text{content}} + \lambda_2 \mathcal{L}_{\text{color}} + \mathcal{L}_{\text{feat}}, \quad (14)$$

where  $\lambda_1$  and  $\lambda_2$  are hyperparameters empirically set to 1e-3 and 100. During the inference stage, only ORM participates in the inference, without requiring SPGRM.

## 4. Experiments

### 4.1. Experimental Settings

**Datasets.** We evaluate the proposed framework on several datasets from various scenes, including Kalantari’s dataset [12], Tel’s dataset [28], and Zhang’s dataset [49]. Kalantari’s dataset is a real captured dataset comprising 74 samples for training and 15 samples for testing, focusing primarily on daytime dynamic scenes. Zhang’s dataset primarily focuses on low-light environments and includes two subsets: BracketIRE and BracketIRE+. BracketIRE contains LDR image sequences with various degradations, while BracketIRE+ extends this by including additional  $4 \times$  super-resolution tasks. Each subset contains 1,045 pairs used for training, and the remaining 290 pairs used for testing. In contrast, Tel’s dataset offers a more balanced distribution of scenes and motions, with samples collected under diverse lighting conditions and encompassing a variety of motion types in equal proportions, with 108 samples for training and 36 for testing. It is worth noting that Kalantari’s and Tel’s datasets are in sRGB format, while Zhang’s dataset uses RAW format.

Methods	Tel’s dataset [28]					Kalantari’s dataset [12]				
	PSNR- $\mu$ $\uparrow$	PSNR-L $\uparrow$	SSIM- $\mu$ $\uparrow$	SSIM-L $\uparrow$	HV2 $\uparrow$	PSNR- $\mu$ $\uparrow$	PSNR-L $\uparrow$	SSIM- $\mu$ $\uparrow$	SSIM-L $\uparrow$	HV2 $\uparrow$
NHDR [38]	36.68	39.61	0.9590	0.9853	65.41	42.41	41.43	0.9877	0.9857	61.21
DHDR [12]	40.05	43.37	0.9794	0.9924	67.09	42.67	41.23	0.9888	0.9846	65.05
HDRGAN [24]	41.87	45.23	0.9832	0.9939	67.03	43.92	41.57	0.9905	0.9865	65.45
DiffHDR [40]	42.19	45.66	0.9843	0.9945	69.88	44.11	41.73	0.9911	0.9885	65.52
HyHDR [39]	-	-	-	-	-	44.64	42.47	0.9915	0.9894	66.05
SCTNet [28]	42.48	47.46	0.9849	0.9952	70.66	44.43	42.21	0.9918	0.9891	66.64
LF-Diff [11]	-	-	-	-	-	44.76	42.59	0.9919	0.9906	66.54
AHDR [37]	41.92	45.20	0.9836	0.9942	67.09	43.62	41.03	0.9900	0.9862	64.60
AHDR+	43.18 <b>+1.26</b>	46.97 <b>+1.77</b>	0.9874 <b>+0.38</b>	0.9955 <b>+0.13</b>	70.39 <b>+3.30</b>	44.24 <b>+0.62</b>	41.54 <b>+0.51</b>	0.9910 <b>+0.10</b>	0.9880 <b>+0.18</b>	65.84 <b>+1.24</b>
HDR-Trans [22]	42.32	46.38	0.9843	0.9948	69.23	44.24	42.17	0.9916	0.9890	66.03
HDR-Trans+	43.38 <b>+1.06</b>	47.85 <b>+1.47</b>	0.9879 <b>+0.36</b>	0.9959 <b>+0.11</b>	70.94 <b>+1.71</b>	44.68 <b>+0.44</b>	42.39 <b>+0.22</b>	0.9918 <b>+0.02</b>	0.9897 <b>+0.07</b>	66.67 <b>+0.64</b>
TMRNet [49]	42.72	45.98	0.9867	0.9953	69.13	43.92	42.09	0.9907	0.9891	65.32
TMRNet+	43.15 <b>+0.43</b>	47.19 <b>+1.21</b>	0.9874 <b>+0.07</b>	0.9961 <b>+0.09</b>	70.59 <b>+1.46</b>	44.49 <b>+0.57</b>	42.39 <b>+0.30</b>	0.9915 <b>+0.08</b>	0.9895 <b>+0.04</b>	66.04 <b>+0.72</b>

Table 1. The evaluation results on Tel’s and Kalantari’s datasets. The improvements brought by our framework to the baseline models are highlighted in red, with the SSIM improvement displayed as  $100\times$  the actual value.

**Evaluation Metrics.** To ensure a fair quantitative comparison, we adhere to the original metrics settings for each dataset. For Zhang’s dataset in RAW format, we use PSNR- $\mu$ , SSIM- $\mu$ , and LPIPS [46] as evaluation metrics. For Kalantari’s and Tel’s datasets in sRGB format, we use PSNR-L, PSNR- $\mu$ , SSIM-L, SSIM- $\mu$ , and HDR-VDP-2 [23]. The subscripts  $\mu$  and L indicate that these metrics are computed in the tonemapped and linear domains.

**Compared Methods.** To verify the effectiveness of our designs, we conduct experiments on four datasets using several well-established HDR reconstruction models. These include AHDR [37], which is representative of CNN-based methods, and HDR-Trans [22], which exemplifies Transformer-based methods. Additionally, we include TMRNet [49], which is currently the SOTA method for HDR image reconstruction and enhancement. We further evaluate our method against a rich collection of SOTA techniques [4, 5, 12, 13, 25, 28, 38]. These models and datasets are carefully selected to cover a range of HDR reconstruction methodologies and scenarios, thereby demonstrating the versatility of our framework.

**Implementation Details.** We train all components of our method simultaneously, utilizing the released code for the baseline networks with consistent training settings. We obtain semantic intermediate features and semantic maps through the frozen, pre-trained FastSAM [50]. The training is conducted using PyTorch in a Python environment, leveraging four NVIDIA Tesla A100 GPUs. We employ the Adam optimizer, configured with  $\beta_1 = 0.9$  and  $\beta_2 = 0.999$ , for optimization. A learning rate of  $2 \times 10^{-4}$  is applied, and each GPU processes a batch size of 16. No-

Methods	BracketIRE [49]	BracketIRE+[49]
	PSNR $\uparrow$ /SSIM $\uparrow$ /LPIPS $\downarrow$	PSNR $\uparrow$ /SSIM $\uparrow$ /LPIPS $\downarrow$
HDRGAN [24]	35.05 / 0.9161 / 0.175	28.35 / 0.8423 / 0.338
BIPNet [4]	35.97 / 0.9314 / 0.145	28.44 / 0.8453 / 0.311
Burstormer [5]	37.01 / 0.9454 / 0.127	28.59 / 0.8516 / 0.292
SCTNet [28]	36.90 / 0.9437 / 0.120	28.28 / 0.8461 / 0.282
Kim [13]	37.93 / 0.9452 / 0.115	28.33 / 0.8494 / 0.270
AHDR [37]	36.32 / 0.9273 / 0.154	28.17 / 0.8422 / 0.309
AHDR+	38.78 / 0.9480 / 0.116 <b>+2.46 / +2.07 / -0.038</b>	30.25 / 0.8696 / 0.274 <b>+2.08 / +2.74 / -0.035</b>
HDR-Trans [22]	36.54 / 0.9341 / 0.127	28.18 / 0.8483 / 0.282
HDR-Trans+	39.09 / 0.9507 / 0.104 <b>+2.55 / +1.66 / -0.023</b>	30.34 / 0.8706 / 0.270 <b>+2.16 / +2.23 / -0.012</b>
TMRNet [49]	38.19 / 0.9488 / 0.112	28.91 / 0.8572 / 0.273
TMRNet+	39.71 / 0.9527 / 0.110 <b>+1.42 / +0.39 / -0.002</b>	30.61 / 0.8723 / 0.269 <b>+1.70 / +1.41 / -0.004</b>

Table 2. The evaluation results on Zhang’s dataset.

tably, the BracketIRE+ dataset from Zhang *et al.* requires an additional super-resolution step. For all baseline models, the *Upsampler* module is implemented using the default method provided in the benchmark [49].

## 4.2. Quantitative Evaluation

**Quantitative results on RAW format dataset.** The evaluation results on Zhang’s dataset are shown in Tab. 2. By introducing the semantic prior of self-distillation learning at the content and color levels, our method provides an average improvement of 2.14/1.98 dB in PSNR on the BracketIRE/BracketIRE+ datasets, respectively. Furthermore, TMRNet+ achieves PSNR values of 39.71/30.61 dB on the

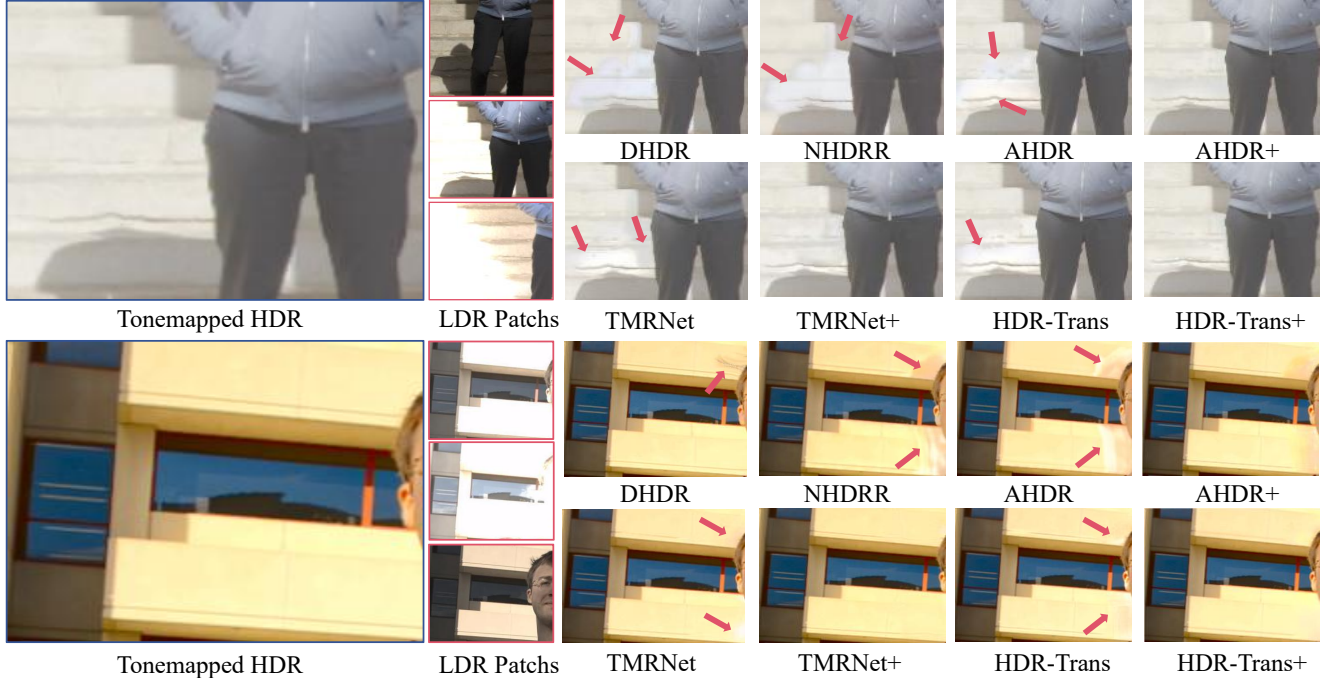


Figure 4. Visual comparison of baseline methods with and without our framework on Tel and Kalantari’s datasets.

BracketIRE/BracketIRE+ datasets, setting a new state-of-the-art benchmark. Furthermore, our framework significantly enhances the SSIM index, underscoring its superior ability to restore the image dynamic range while maintaining structural integrity and fine details. Additionally, the notable increase in LPIPS scores, facilitated by our framework, demonstrates a closer alignment with human perceptual judgment. This is achieved through the innovative incorporation of semantic priors into our design.

**Quantitative results on sRGB format dataset.** The evaluation results on Tel’s and Kalantari’s datasets are shown in Tab. 1. We can observe that our framework effectively boosts the performance of baseline methods, providing an average improvement of 0.91/0.54 dB in PSNR on the Kalantari/Tel’s datasets, respectively. The PSNR improvement on the Kalantari’s dataset is only half that of the Tel’s dataset. This is because, compared to the Tel’s dataset, the Kalantari’s dataset primarily focuses on daytime dynamic scenes, where input images typically do not contain degradations, which are the main factors addressed by semantic priors. However, our proposed framework consistently improves the baseline’s performance. Through consistent and stable performance enhancements across multiple scene datasets, our framework demonstrates its effectiveness and flexibility.

### 4.3. Qualitative Evaluation

**Qualitative results on bright scenes.** Reconstructing HDR images in dynamic bright scenes often causes ghosting arti-

facts when essential content (*e.g.*, content, details) for over-exposed areas is missing due to object or camera movement. Fig. 4 showcases qualitative results for bright scenes from the two datasets. Our framework is applied to multiple baseline models and compared with various state-of-the-art approaches using test data from the Kalantari’s (top row) and Tel’s (bottom row) datasets, which include challenging samples characterized by saturated backgrounds and foreground motions. As shown in the top row of Fig. 4, all baseline results exhibit noticeable artifacts in the step regions, whereas our proposed framework significantly suppresses ghosting phenomena. In the bottom row, all improved methods except AHDR+ eliminate ghosting, but AHDR+ still shows a significant reduction in ghosting compared to the baselines. This demonstrates the effectiveness of our framework in removing or suppressing ghosting caused by missing information.

**Qualitative results on low-light scenes.** Captured LDR images often suffer from noticeable degradation in low-light scenes, which significantly affects the final reconstruction quality. Fig. 5 showcases qualitative results from the BracketIRE (left) and BracketIRE+ (right) datasets. As shown in the left part, the LDR images contain noticeable degradations, and all methods exhibit unclear details. Our proposed framework significantly enhances the model’s detail representation, reducing the impact of image degradations. For example, the tigers and stars within the blue boxes exhibit clearer textures. Furthermore, compared to BracketIRE, the LDR images in BracketIRE+ have lower resolution, posing

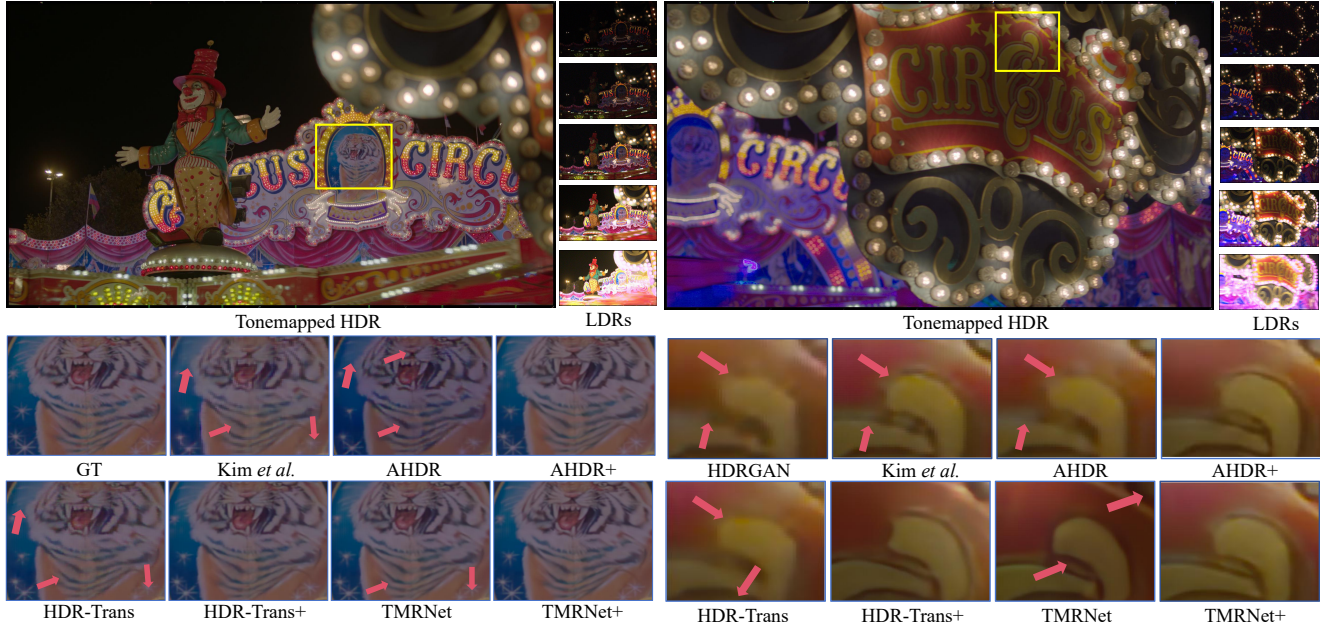


Figure 5. Visual comparison of baseline methods with and without our framework on BracketIRE and BracketIRE+ datasets.

Method	ORM Results		SPGRM Results	
	PSNR- $\mu$ $\uparrow$	SSIM- $\mu$ $\uparrow$	PSNR- $\mu$ $\uparrow$	SSIM- $\mu$ $\uparrow$
AHDR	41.92	0.9836	-	-
w/o $\mathcal{L}_{\text{content}}$	42.15	0.9841	42.69	0.9849
w/o $\mathcal{L}_{\text{color}}$	43.09	0.9861	43.19	0.9864
w/o SKAM	43.11	0.9862	43.13	0.9873
w/o FastSAM	41.86	0.9829	41.86	0.9830
w HRNet	42.95	0.9859	42.95	0.9859
<b>AHDR+</b>	<b>43.18</b>	<b>0.9874</b>	<b>43.18</b>	<b>0.9874</b>

Table 3. Ablation studies of proposed framework.

a challenge for reconstructing high-quality HDR images. As shown in the right part, all baseline models almost fail to restore realistic textures and show significant blurring. In contrast, our proposed framework significantly improves the imaging quality of the baseline models, recovering the scene’s outlines and details more completely.

#### 4.4. Ablation Studies

Considering that Tel’s dataset offers a more balanced distribution of scenes and motions, We conduct ablation experiments on this dataset to validate the effectiveness of our proposed method. From Tab. 3, we can observe that the absence of any component in the semantic knowledge transfer scheme leads to a noticeable drop in performance. Specifically,  $\mathcal{L}_{\text{content}}$  as the foundational loss function for self-distillation, has a significant impact on model performance. In other words, the proposed  $\mathcal{L}_{\text{color}}$  effectively enhances the self-distillation capability when built upon the base loss function. W/o SKAM refers to the variant where the semantic knowledge alignment module is removed. We ob-

serve that this variation slightly degrades the performance of ORM, indicating that SKAM contributes to effective semantic knowledge transfer. Furthermore, w/o FastSAM indicates the removal of semantic priors in the SPGRM, instead employing a simple second-stage enhancement. We discover that merely increasing the model’s parameter count does not lead to substantial performance gains and may even cause overfitting, resulting in performance degradation. In addition, we assess the influence of diverse semantic priors derived from FastSAM and the widely utilized HRNet [30]. Given that SAM-based method offers richer and more nuanced semantic information across multiple scales, our approach outperforms HRNet that relies solely on semantic cues from instance and category labels.

#### 5. Conclusion

Existing multi-exposure HDR imaging methods primarily focus on mitigating artifact issues caused by motion, but they overlook the inherently ill-posed nature of captured LDR images in real-world scenarios. To tackle these challenges, we introduces a general framework that leverages semantic priors from pretrained segmentation models to boost existing HDR reconstruction models without modifying the original network. By endowing models with semantic knowledge, our framework enables a deeper understanding of image content, providing explicit guidance for the reconstruction process. Extensive experiments demonstrate that the proposed framework consistently improves the performance of multiple baseline models, achieving state-of-the-art results across diverse datasets encompassing various scenes and formats.

## References

- [1] Andreas Aakerberg, Anders S Johansen, Kamal Nasrollahi, and Thomas B Moeslund. Semantic segmentation guided real-world super-resolution. In *Proceedings of the IEEE/CVF Winter Conference on Applications of Computer Vision*, pages 449–458, 2022. 2
- [2] Jie Chen, Zaifeng Yang, Tsz Nam Chan, Hui Li, Junhui Hou, and Lap-Pui Chau. Attention-guided progressive neural texture fusion for high dynamic range image restoration. *IEEE Transactions on Image Processing*, 31:2661–2672, 2022. 2
- [3] Rufeng Chen, Bolun Zheng, Hua Zhang, Quan Chen, Chenggang Yan, Gregory Slabaugh, and Shanxin Yuan. Improving dynamic hdr imaging with fusion transformer. In *Proceedings of the AAAI Conference on Artificial Intelligence*, pages 340–349, 2023. 1, 2
- [4] Akshay Dudhane, Syed Waqas Zamir, Salman Khan, Fahad Shahbaz Khan, and Ming-Hsuan Yang. Burst image restoration and enhancement. In *Proceedings of the IEEE/CVF Conference on Computer Vision and Pattern Recognition*, pages 5759–5768, 2022. 6
- [5] Akshay Dudhane, Syed Waqas Zamir, Salman Khan, Fahad Shahbaz Khan, and Ming-Hsuan Yang. Burstformer: Burst image restoration and enhancement transformer. In *2023 IEEE/CVF Conference on Computer Vision and Pattern Recognition (CVPR)*, pages 5703–5712. IEEE, 2023. 6
- [6] Minhao Fan, Wenjing Wang, Wenhao Yang, and Jiaying Liu. Integrating semantic segmentation and retinex model for low-light image enhancement. In *Proceedings of the 28th ACM international conference on multimedia*, pages 2317–2325, 2020. 2
- [7] Li Fang, Qian Wang, and Long Ye. Glnet: light field angular superresolution with arbitrary interpolation rates. *Visual Intelligence*, 2(1):6, 2024. 2
- [8] Kaiming He, Xinlei Chen, Saining Xie, Yanghao Li, Piotr Dollár, and Ross Girshick. Masked autoencoders are scalable vision learners. In *Proceedings of the IEEE/CVF conference on computer vision and pattern recognition*, pages 16000–16009, 2022. 2
- [9] YongSeok Heo, KyoungMu Lee, SangUk Lee, Youngsu Moon, and Joonhyuk Cha. Ghost-free high dynamic range imaging. In *IEEE Conference on Asian Conference on Computer Vision (ACCV)*, pages 486–500, 2011. 2
- [10] Jun Hu, O. Gallo, K. Pulli, and Xiaobai Sun. HDR deghosting: How to deal with saturation? In *IEEE Conference on Computer Vision and Pattern Recognition (CVPR)*, pages 1163–1170, 2013. 2
- [11] Tao Hu, Qingsen Yan, Yuankai Qi, and Yanning Zhang. Generating content for hdr deghosting from frequency view. In *Proceedings of the IEEE/CVF Conference on Computer Vision and Pattern Recognition*, pages 25732–25741, 2024. 2, 6
- [12] Nima Khademi Kalantari and Ravi Ramamoorthi. Deep high dynamic range imaging of dynamic scenes. *ACM Transactions on Graphics*, 36(4):1–12, 2017. 1, 2, 5, 6
- [13] Jungwoo Kim and Min H Kim. Joint demosaicing and deghosting of time-varying exposures for single-shot hdr imaging. In *Proceedings of the IEEE/CVF International Conference on Computer Vision*, pages 12292–12301, 2023. 6
- [14] Lingtong Kong, Bo Li, Yike Xiong, Hao Zhang, Hong Gu, and Jinwei Chen. Safnet: Selective alignment fusion network for efficient hdr imaging. In *Proceedings of the European Conference on Computer Vision (ECCV)*, 2024. 2
- [15] Simiao Li, Yun Zhang, Wei Li, Hanting Chen, Wenjia Wang, Bingyi Jing, Shaohui Lin, and Jie Hu. Knowledge distillation with multi-granularity mixture of priors for image super-resolution. *arXiv preprint arXiv:2404.02573*, 2024. 5
- [16] Xiaoming Li, Chaofeng Chen, Shangchen Zhou, Xianhui Lin, Wangmeng Zuo, and Lei Zhang. Blind face restoration via deep multi-scale component dictionaries. In *European conference on computer vision*, pages 399–415. Springer, 2020. 2
- [17] Yi Li, Yi Chang, Changfeng Yu, and Luxin Yan. Close the loop: A unified bottom-up and top-down paradigm for joint image deraining and segmentation. In *Proceedings of the AAAI Conference on Artificial Intelligence*, pages 1438–1446, 2022. 2
- [18] Dong Liang, Ling Li, Mingqiang Wei, Shuo Yang, Liyan Zhang, Wenhao Yang, Yun Du, and Huiyu Zhou. Semantically contrastive learning for low-light image enhancement. In *Thirty-Sixth AAAI Conference on Artificial Intelligence, AAAI 2022, Thirty-Fourth Conference on Innovative Applications of Artificial Intelligence, IAAI 2022, The Twelfth Symposium on Educational Advances in Artificial Intelligence, EAAI 2022 Virtual Event, February 22 - March 1, 2022*, pages 1555–1563. AAAI Press, 2022. 1, 2
- [19] Tsung-Yi Lin, Piotr Dollár, Ross Girshick, Kaiming He, Bharath Hariharan, and Serge Belongie. Feature pyramid networks for object detection. In *Proceedings of the IEEE conference on computer vision and pattern recognition*, pages 2117–2125, 2017. 4
- [20] Ding Liu, Bihan Wen, Xianming Liu, Zhangyang Wang, and Thomas S. Huang. When image denoising meets high-level vision tasks: A deep learning approach. In *IJCAI*, 2018. 2
- [21] Shuaizheng Liu, Xindong Zhang, Lingchen Sun, Zhetong Liang, Hui Zeng, and Lei Zhang. Joint hdr denoising and fusion: A real-world mobile hdr image dataset. In *Proceedings of the IEEE/CVF Conference on Computer Vision and Pattern Recognition*, pages 13966–13975, 2023. 2
- [22] Zhen Liu, Yinglong Wang, Bing Zeng, and Shuaicheng Liu. Ghost-free high dynamic range imaging with context-aware transformer. In *Computer Vision - ECCV 2022 - 17th European Conference, Tel Aviv, Israel, October 23-27, 2022, Proceedings, Part XIX*, pages 344–360. Springer, 2022. 1, 6
- [23] Rafat Mantiuk, Kil Joong Kim, Allan G. Rempel, and Wolfgang Heidrich. HDR-VDP-2: a calibrated visual metric for visibility and quality predictions in all luminance conditions. In *ACM Siggraph*, pages 1–14, 2011. 6
- [24] Yuzhen Niu, Jianbin Wu, Wenxi Liu, Wenzhong Guo, and Rynson WH Lau. Hdr-gan: Hdr image reconstruction from multi-exposed ldr images with large motions. *IEEE Transactions on Image Processing*, 30:3885–3896, 2021. 2, 6
- [25] Yuzhen Niu, Jianbin Wu, Wenxi Liu, Wenzhong Guo, and Rynson W. H. Lau. HDR-GAN: HDR image reconstruction

- from multi-exposed LDR images with large motions. *IEEE Trans. Image Process.*, 30:3885–3896, 2021. 1, 6
- [26] Pradeep Sen, Nima Khademi Kalantari, Maziar Yaesoubi, Soheil Darabi, Dan B Goldman, and Eli Shechtman. Robust patch-based hdr reconstruction of dynamic scenes. *ACM Trans. Graph.*, 31(6):203–1, 2012. 2
- [27] Jou Won Song, Ye-In Park, Kyeongbo Kong, Jaeho Kwak, and Suk-Ju Kang. Selective transhdr: Transformer-based selective hdr imaging using ghost region mask. In *Computer Vision–ECCV 2022: 17th European Conference, Tel Aviv, Israel, October 23–27, 2022, Proceedings, Part XVII*, pages 288–304. Springer, 2022. 1, 2
- [28] Steven Tel, Zongwei Wu, Yulun Zhang, Barthélemy Heyrman, Cédric Demonceaux, Radu Timofte, and Dominique Ginhac. Alignment-free hdr deghosting with semantics consistent transformer. In *Proceedings of the IEEE/CVF International Conference on Computer Vision (ICCV)*, pages 12836–12845, 2023. 1, 2, 5, 6
- [29] Anna Tomaszewska and Radoslaw Mantiuk. Image registration for multi-exposure high dynamic range image acquisition. In *International Conference in Central Europe on Computer Graphics and Visualization, WSCG’07, 2007*. 2
- [30] Jingdong Wang, Ke Sun, Tianheng Cheng, Borui Jiang, Chaorui Deng, Yang Zhao, Dong Liu, Yadong Mu, Minghui Tan, Xinggang Wang, et al. Deep high-resolution representation learning for visual recognition. *IEEE transactions on pattern analysis and machine intelligence*, 43(10):3349–3364, 2020. 8
- [31] Lin Wang and Kuk-Jin Yoon. Deep learning for hdr imaging: State-of-the-art and future trends. *IEEE Transactions on Pattern Analysis and Machine Intelligence*, 2021. 1
- [32] Xintao Wang, Ke Yu, Chao Dong, and Chen Change Loy. Recovering realistic texture in image super-resolution by deep spatial feature transform. In *Proceedings of the IEEE conference on computer vision and pattern recognition*, pages 606–615, 2018. 1, 2
- [33] Greg Ward. Fast, robust image registration for compositing high dynamic range photographs from hand-held exposures. *Journal of Graphics Tools*, 8, 2012. 2
- [34] Yuhui Wu, Chen Pan, Guoqing Wang, Yang Yang, Jiwei Wei, Chongyi Li, and Heng Tao Shen. Learning semantic-aware knowledge guidance for low-light image enhancement. In *Proceedings of the IEEE/CVF Conference on Computer Vision and Pattern Recognition*, pages 1662–1671, 2023. 1, 2
- [35] Gangwei Xu, Yujin Wang, Jinwei Gu, Tianfan Xue, and Xin Yang. Hdrflow: Real-time hdr video reconstruction with large motions. In *Proceedings of the IEEE/CVF Conference on Computer Vision and Pattern Recognition*, pages 24851–24860, 2024. 2
- [36] Qingsen Yan, Jinqiu Sun, Haisen Li, Yu Zhu, and Yanning Zhang. High dynamic range imaging by sparse representation. *Neurocomputing*, 269:160–169, 2017. 2
- [37] Qingsen Yan, Dong Gong, Qinfeng Shi, Anton van den Hengel, Chunhua Shen, Ian Reid, and Yanning Zhang. Attention-guided network for ghost-free high dynamic range imaging. In *Proceedings of the IEEE/CVF Conference on Computer Vision and Pattern Recognition*, pages 1751–1760, 2019. 1, 2, 6
- [38] Qingsen Yan, Lei Zhang, Yu Liu, Yu Zhu, Jinqiu Sun, Qinfeng Shi, and Yanning Zhang. Deep hdr imaging via a non-local network. *IEEE Transactions on Image Processing*, 29:4308–4322, 2020. 6
- [39] Qingsen Yan, Weiye Chen, Song Zhang, Yu Zhu, Jinqiu Sun, and Yanning Zhang. A unified hdr imaging method with pixel and patch level. In *Proceedings of the IEEE/CVF Conference on Computer Vision and Pattern Recognition*, pages 22211–22220, 2023. 2, 6
- [40] Qingsen Yan, Tao Hu, Yuan Sun, Hao Tang, Yu Zhu, Wei Dong, Luc Van Gool, and Yanning Zhang. Towards high-quality hdr deghosting with conditional diffusion models. *IEEE Transactions on Circuits and Systems for Video Technology*, pages 1–1, 2023. 2, 6
- [41] Qingsen Yan, Kangzhen Yang, Tao Hu, Gengqiang Chen, Kexin Dai, Peng Wu, Wenqi Ren, and Yanning Zhang. From dynamic to static: Stepwisely generate hdr image for ghost removal. *IEEE Transactions on Circuits and Systems for Video Technology*, 2024. 2
- [42] Adriano Z Zambom and Ronaldo Dias. A review of kernel density estimation with applications to econometrics. *International Econometric Review*, 5(1):20–42, 2013. 4
- [43] Syed Waqas Zamir, Aditya Arora, Salman Khan, Munawar Hayat, Fahad Shahbaz Khan, and Ming-Hsuan Yang. Restormer: Efficient transformer for high-resolution image restoration. In *Proceedings of the IEEE/CVF conference on computer vision and pattern recognition*, pages 5728–5739, 2022. 4
- [44] Linfeng Zhang, Chenglong Bao, and Kaisheng Ma. Self-distillation: Towards efficient and compact neural networks. *IEEE Transactions on Pattern Analysis and Machine Intelligence*, 44(8):4388–4403, 2021. 2
- [45] Quan Zhang, Xiaoyu Liu, Wei Li, Hanting Chen, Junchao Liu, Jie Hu, Zhiwei Xiong, Chun Yuan, and Yunhe Wang. Distilling semantic priors from sam to efficient image restoration models. In *Proceedings of the IEEE/CVF Conference on Computer Vision and Pattern Recognition*, pages 25409–25419, 2024. 1, 2
- [46] Richard Zhang, Phillip Isola, Alexei A Efros, Eli Shechtman, and Oliver Wang. The unreasonable effectiveness of deep features as a perceptual metric. In *Proceedings of the IEEE conference on computer vision and pattern recognition*, pages 586–595, 2018. 6
- [47] Xiang Zhang, Qiang Zhu, Tao Hu, and Qingsen Yan. Eifhldr: An efficient network for multi-exposure high dynamic range imaging. In *ICASSP 2024 - 2024 IEEE International Conference on Acoustics, Speech and Signal Processing (ICASSP)*, pages 6560–6564, 2024. 2
- [48] Zhao Zhang, Huan Zheng, Richang Hong, Mingliang Xu, Shuicheng Yan, and Meng Wang. Deep color consistent network for low-light image enhancement. In *Proceedings of the IEEE/CVF conference on computer vision and pattern recognition*, pages 1899–1908, 2022. 4
- [49] Zhilu Zhang, Shuohao Zhang, Renlong Wu, Zifei Yan, and Wangmeng Zuo. Exposure bracketing is all you need for a high-quality image. In *ICLR*, 2025. 1, 5, 6

- [50] Xu Zhao, Wenchao Ding, Yongqi An, Yinglong Du, Tao Yu, Min Li, Ming Tang, and Jinqiao Wang. Fast segment anything, 2023. [4](#), [6](#)
- [51] Shen Zheng and Gaurav Gupta. Semantic-guided zero-shot learning for low-light image/video enhancement. In *Proceedings of the IEEE/CVF Winter conference on applications of computer vision*, pages 581–590, 2022. [2](#)
- [52] Yunhao Zou, Chenggang Yan, and Ying Fu. Rawhdr: High dynamic range image reconstruction from a single raw image. In *Proceedings of the IEEE/CVF International Conference on Computer Vision*, pages 12334–12344, 2023. [2](#)